A Branching Particle-based Nonlinear Filter for Multi-target Tracking

David J. Ballantyne
University of Alberta
Edmonton, AB, Canada
dballant@math.ualberta.ca

Hubert Y. Chan
University of Alberta
Edmonton, AB, Canada
hubert@math.ualberta.ca

Michael A. Kouritzin
University of Alberta
Edmonton, AB, Canada
mkouritz@math.ualberta.ca

Abstract – *A branching particle-based filter is used to detect and track multiple simulated maneuvering ships in a region of water. The ship trajectories exhibit nonlinear dynamics and interact in a nonlinear manner so that the ships do not collide. There is no a priori knowledge of the number of ships in the region. Observations model a sensor tracking the ships from above the region as in a low observable problem.*

The branching filter simulates particles, each of which is a sample from the domain of possible combinations of ship number and the state of those ships, and each of which is evolved independently using the stochastic law of the signal between observations. The branching filter employs these particles to provide the approximated conditional distribution of the signal in the combined domain, given all observations. Quantitative results recording the capacity of the branching filter to determine the number of ships in the region and the location of each ship are presented.

Keywords: Tracking, particle-based filtering, multiple target, branching filter.

1 Introduction

Properly designed adaptive particle systems provide versatile yet under-exploited methods for asymptotic solutions to filtering problems. Hitherto, most practical models have concentrated on the single target scenario. However, the merits of particle systems may be best illustrated in the perennially problematic multiple-target problems. Del Moral and Salut[3] describe the adaptive particle system approach to filtering; our branching method was introduced by Kouritzin and first discussed in Ballantyne, Chan, and Kouritzin [1]; and Salmond and Gordon[8] and Hue, Le Cadre, and Pérez[5] have used particle systems in multiple target problems. Our approach is different than that of Hue et. al. in that the filter is constructed directly by expanding the domain of the signal, rather than introducing Gibbs sampling, and can thus readily handle cases in which the initial number of targets is unknown and that number may change over time.

It can be critical in applications to determine how many, if any, targets are located in a region of space based upon a noisy, corrupted sequence of observations. In this paper, we address this problem for multiple interacting targets diffusing in a plane and spatial observations with high noise intensity. For example, Figure 1 depicts our particle system filter trying to detect and track possible targets (in the top left frame) based upon observations corrupted by extreme noise (as shown in the top middle frame). The estimated locations of the targets given that there are one, two, or three targets to track are displayed in the lower left, middle, and right frames, and a greater length of a bar along the bottom of each of these frames indicates a greater estimated probability that the signal contains that number of targets. Any or all of the target locations may not closely represent an actual target, but rather be an artifact of the observation noise.

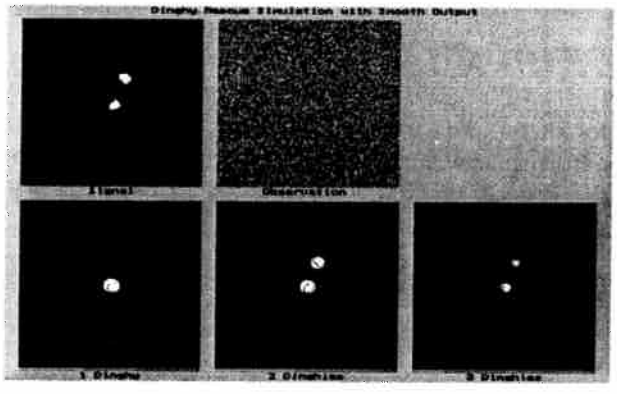

Figure 1: Example multi-target filter

How does one best decide how many targets really exist in the viewing area? In the case that the targets act independently or interact weakly, this question can be answered by imbedding the targets into a measure-valued Markov process. Since we are filtering measures rather

than a single target we quickly review the theory of filtering for signals in Polish spaces.

1.1 Filtering continuous Markov signals

Suppose $(\Omega, \mathcal{F}, P)$ is a probability space, S is a complete, separable metric space, and $B(S)$ is the set of bounded, measurable functions on S. Then, $\mathbb{X}$ is a cadlag homogeneous (L, P_0)-Markov process on S if: $t \to \mathbb{X}_t(\omega)$ is right continuous with left hand limits for each ω, $P(\mathbb{X}_0 \in B) = P_0(B)$ for all $B \in \mathcal{B}(S)$ (the Borel σ-field of S), $P(\mathbb{X}_{t+s} \in B | \sigma\{\mathbb{X}_u, u \le t\}) = P(\mathbb{X}_{t+s} \in B | \mathbb{X}_t)$ for sets $B \in \mathcal{B}(S)$, and

$$E[f(\mathbb{X}_t)] = E[f(\mathbb{X}_0)] + \int_0^t E[Lf(\mathbb{X}_s)]ds \quad (1)$$

for all bounded measurable functions $f \in D(L) \subset B(S)$, the (weak) domain of L. Suppose further that this signal cannot be measured directly, but rather only through an imperfect sensor. In particular, it is common to assume that the observations occur at times t_k and take the form

$$Y_k = H_k(\mathbb{X}_{t_k}, V_k), \ \forall k = 1, 2, ..., \quad (2)$$

where $\{V_k, \ k = 1, 2, ...\}$ is an independent vector-valued noise sequence.

Then, the conditional distribution p_t^Y of $\mathbb{X}_t$ given Y_k, $t_k \le t$ is solved by Bayes' rule

$$p_t^Y(f) = E(f(\mathbb{X}_t) | Y_{t_1}, ..., Y_{t_k}) = \frac{\overline{p}_t^Y(f)}{\overline{p}_t^Y(1)}, \quad \forall f \in D(L), \quad (3)$$

where (under some mild assumptions on H_k and V_k) the unnormalized conditional distribution $\overline{p}_t^Y$ is the unique solution to

$$\overline{p}_t^Y(f) - \overline{p}_0^Y(f) - \int_0^t \overline{p}_s^Y(Lf)ds = M_t(f) \quad a.s. \quad (4)$$

for all $f \in D(L)$. Here, for each $f \in D(L)$, $M_t(f)$ is a martingale with respect to the filtration $\sigma\{Y_{t_i}, t_i \le t\}$ that depends on the H_k, ϕ_k, and Y_k. Branching particle methods approximate the solution to Equation (4).

2 Signal description

Suppose N is a non-negative integer-valued random variable, (S_0, d_0) is some complete, separable metric space, and $\mathcal{B}$ be the Borel σ-field for S_0. For example, $S_0 = \mathbb{R}^6 \times \{1, 2, 3\}$ with Euclidean distance $|\cdot|$ in the following. We let S denote the space of finite, non-negative measures μ on S_0, metrized by the extended Prohorov distance

$$d(\mu, \nu) \doteq \inf\{\varepsilon > 0 : \mu(B) \le \nu(B^\varepsilon) + \varepsilon, \ \nu(B) \le \mu(B^\varepsilon) + \varepsilon \ \forall B \in \mathcal{B}\}, \quad (5)$$

where $B^\varepsilon \doteq \{x \in S_0 : d_0(x, y) < \varepsilon \text{ for some } y \in B\}$. Then, (S, d) is also a complete, separable metric space.

Our signal measure is a homogeneous Markov process $\mathbb{X}$ on S constructed as

$$\mathbb{X}_t(B) = \sum_{i=1}^{N_t} \delta_{X_t^i}(B) = \text{Number of targets in } B, \quad (6)$$

where N_t is the random number of targets depending on t. Inasmuch as it is vital that $\mathbb{X}_t$ is a Markov process, we consider the case in which N_t is decreasing through the removal of targets to a cemetery state when they leave a bounded portion of the target domain, and we limit possible target interactions to weak interactions, meaning those that can be represented in terms of $\mathbb{X}_t$ itself. In this case, $\mathbb{X}$ is a $(P_0, \mathcal{L})$-Markov process, where P_0 is the initial signal measure and the operator $\mathcal{L}$ describes the probabilistic evolution of the signal. The weak interactions are designed to repel nearby targets in order to avoid collisions and to attract distant targets. This is enforced indirectly by increasing the probability that the orientation change of a target is away from other close targets, and increasing the probability that the orientation change of a target is towards other distant targets. Our model thereby reflects loose coordination of the targets.

2.1 Target models with interactions

We assume that there is a random number N_t of targets, where $N_t \in \{0, 1, 2, 3\}$. Each target has seven state variables: (x_t^i, y_t^i) and $(\dot{x}_t^i, \dot{y}_t^i)$ denote the current planar location and velocity, respectively, of the i^{th} target; θ_t^i and $\dot{\theta}_t^i$ are the orientation and angular velocity; and χ_t^i denotes the current maneuver type from the possible set of {drifting, rowing, motoring}. We use the notation $X_t^i \doteq (x_t^i, y_t^i, \theta_t^i, \dot{x}_t^i, \dot{y}_t^i, \dot{\theta}_t^i, \chi_t^i)$ for the state of target i and $\mathbb{X}_t(\cdot) = \sum_{i=1}^{N_t} \delta_{X_t^i}(\cdot)$ for the signal measure. In order to write the stochastic equations for these variables we let $\{B^{i,a}, B^{i,b}, B^{i,c}\}_{i=1}^{N_t}$ be independent standard Brownian motions with dimension three, two, and two. Also, we define the following attraction-repulsion field:

$$\kappa(s_1, s_2) = \begin{cases} 0 & s_1 = s_2 \\ \frac{\Pi(s_1, s_2)}{1000N} - \frac{3}{4(\Pi(s_1, s_2) - \varepsilon)} & s_1 \neq s_2 \end{cases}, \quad (7)$$

$$\kappa_x(s_1, s_2) = \kappa(s_1, s_2) \frac{\pi_x(s_1) - \pi_x(s_2)}{\Pi(s_1, s_2)}, \quad (8)$$

and

$$\kappa_y(s_1, s_2) = \kappa(s_1, s_2) \frac{\pi_y(s_1) - \pi_y(s_2)}{\Pi(s_1, s_2)} \quad (9)$$

for all ships $s_1, s_2 \in S_0 = \mathbb{R}^6 \times \{1, 2, 3\}$, where

$$\Pi(s_1, s_2) = \sqrt{|\pi_x(s_1) - \pi_x(s_2)|^2 + |\pi_y(s_1) - \pi_y(s_2)|^2}, \quad (10)$$

and π_x, π_y denote projection onto the x and y components. The effect of this field, when incorporated into the stochastic Itô equations that describe the motion of the individual targets, is to draw a target slightly towards the pack if it is distant and to repel it from any one other target to which it becomes too close. The value $\epsilon = 13$ represents the closest distance that two targets should come to each other. We define the following variables to enact this attraction-repulsion:

$$\phi_t^{r,i} = \sqrt{\int \left|\kappa(z, X_t^i)\right|^2 \mathbb{X}_t(dz)}, \tag{11}$$

and

$$\phi_t^{\theta,i} = \arctan\Big(\int \kappa_y(z, X_t^i)\mathbb{X}_t(dz), \int \kappa_x(z, X_t^i)\mathbb{X}_t(dz)\Big), \tag{12}$$

which represent the strength and orientation of the deflecting force, and both of which decompose into sums over the finite set of targets.

2.2 Maneuver type

The target state variable χ_t^i is a Markov chain with state space $\{1, 2, 3\}$, representing adrift, rowing, and motoring respectively. The rates are given by:

$$\lambda_{i,t}^{1\to 3}(X_t^i, \mathbb{X}_t) = \lambda_{i,t}^{2\to 3}(X_t^i, \mathbb{X}_t) = 100\phi_t^{r,i}, \tag{13}$$

$$\lambda_{i,t}^{1\to 2}(X_t^i, \mathbb{X}_t) = \lambda_{i,t}^{2\to 1}(X_t^i, \mathbb{X}_t) = \frac{3}{10}, \tag{14}$$

and

$$\lambda_{i,t}^{3\to 1}(X_t^i, \mathbb{X}_t) = \lambda_{i,t}^{3\to 2}(X_t^i, \mathbb{X}_t) = \frac{1}{200\phi_t^{r,i}}. \tag{15}$$

Since the attraction-repulsion field only affects the motion of a target if it is motorized, a strong field increases the likelihood that the target will switch into, or stay in, the motorized maneuver.

The differential equations describing the motion of target i depend on the maneuver type χ_t^i, as follows:

1. *Adrift* ($\chi_t^i = 1$) In this case,

$$d\begin{bmatrix}\dot{x}_t^i \\ \dot{y}_t^i \\ \dot{\theta}_t^i\end{bmatrix} = \begin{bmatrix}\mathfrak{F}_{\dot{x}}(\dot{x}_t^i, \dot{y}_t^i, \theta_t^i) \\ \mathfrak{F}_{\dot{y}}(\dot{x}_t^i, \dot{y}_t^i, \theta_t^i) \\ \mathfrak{F}_{\dot{\theta}}(\dot{x}_t^i, \dot{y}_t^i, \dot{\theta}_t^i, \theta_t^i)\end{bmatrix} dt + \begin{bmatrix}1 & 0 & 0 \\ 0 & 1 & 0 \\ 0 & 0 & 0.5\end{bmatrix} dB_t^{i,a}, \tag{16}$$

where $B_t^{i,a}$ is a three-dimensional standard Brownian motion mentioned previously. To make the simulation more realistic, friction $\mathfrak{F}(\cdot)$ is included in the equation. The calculation of this friction is similar for each motion type and is described below.

2. *Rowing* ($\chi_t^i = 2$) In this case,

$$\begin{bmatrix}\dot{x}_t^i \\ \dot{y}_t^i\end{bmatrix} = \begin{bmatrix}\dot{f}_t^i \cos\theta_t^i \\ \dot{f}_t^i \sin\theta_t^i\end{bmatrix}, \tag{17}$$

where $\dot{f}_t^i$ represents scalar velocity in the forward direction, with

$$d\begin{bmatrix}\dot{f}_t^i \\ \dot{\theta}_t^i\end{bmatrix} = \begin{bmatrix}(3.5 - \dot{f}_t^i + \mathfrak{F}_{\dot{f}}(\dot{x}_t^i, \dot{y}_t^i, \theta_t^i)) \\ \mathfrak{F}_{\dot{\theta}}(\dot{x}_t^i, \dot{y}_t^i, \dot{\theta}_t^i, \theta_t^i)\end{bmatrix} dt + \begin{bmatrix}\sqrt{(4 - \dot{f}_t^i)(\dot{f}_t^i - 3)} & 0 \\ 0 & 0.4\end{bmatrix} dB_t^{i,b}, \tag{18}$$

where $B_t^{i,b}$ is a two-dimensional standard Brownian motion.

3. *Motorized* ($\chi_t^i = 3$) In this case,

$$\begin{bmatrix}\dot{x}_t^i \\ \dot{y}_t^i\end{bmatrix} = \begin{bmatrix}\dot{f}_t^i \cos\theta_t^i \\ \dot{f}_t^i \sin\theta_t^i\end{bmatrix}, \tag{19}$$

where $\dot{f}_t^i$ represents scalar velocity in the forward direction, with

$$d\begin{bmatrix}\dot{f}_t^i \\ \dot{\theta}_t^i\end{bmatrix} = \begin{bmatrix}(9.5 - \dot{f}_t^i + \mathfrak{F}_{\dot{f}}(\dot{x}_t^i, \dot{y}_t^i, \theta_t^i)) \\ (\phi_t^{\theta,i} - \dot{\theta}_t^i)\phi_t^{r,i} + \mathfrak{F}_{\dot{\theta}}(\dot{x}_t^i, \dot{y}_t^i, \dot{\theta}_t^i, \theta_t^i)\end{bmatrix} dt + \begin{bmatrix}\sqrt{(10 - \dot{f}_t^i)(\dot{f}_t^i - 9)} & 0 \\ 0 & 0.4\end{bmatrix} dB_t^{i,c}, \tag{20}$$

where $B_t^{i,c}$ is a two-dimensional standard Brownian motion.

Friction is calculated according to the following model:

$$\mathfrak{F}_{\dot{x}}(\dot{x}, \dot{y}, \theta) = \begin{cases} -\frac{\dot{x}\sqrt{\dot{x}^2+\dot{y}^2}}{\mathfrak{F}_r(\dot{x},\dot{y},\theta)} \cdot f_\ell & \text{if } \dot{x} \neq 0, \dot{y} \neq 0 \\ 0 & \text{if } \dot{x} = \dot{y} = 0 \end{cases}, \tag{21}$$

$$\mathfrak{F}_{\dot{y}}(\dot{x}, \dot{y}, \theta) = \begin{cases} -\frac{\dot{y}\sqrt{\dot{x}^2+\dot{y}^2}}{\mathfrak{F}_r(\dot{x},\dot{y},\theta)} \cdot f_\ell & \text{if } \dot{x} \neq 0, \dot{y} \neq 0 \\ 0 & \text{if } \dot{x} = \dot{y} = 0 \end{cases}, \tag{22}$$

$$\mathfrak{F}_r(\dot{x},\dot{y},\theta) = \sqrt{\begin{array}{l}(\dot{x}\cdot\cos\theta + \dot{y}\cdot\sin\theta)^2 \\ \quad + \frac{1}{4}\cdot(\dot{y}\cdot\cos\theta - \dot{x}\cdot\sin\theta)^2\end{array}}, \quad (23)$$

$$\mathfrak{F}_f(\dot{x},\dot{y},\theta) = \sqrt{\mathfrak{F}_{\dot{x}}(\dot{x},\dot{y},\theta)^2 + \mathfrak{F}_{\dot{y}}(\dot{x},\dot{y},\theta)^2}, \quad (24)$$

and

$$\mathfrak{F}_{\dot{\theta}}(\dot{x},\dot{y},\dot{\theta},\theta) = -\dot{\theta} f_\theta, \quad (25)$$

where f_ℓ and f_θ are constant parameters indicating the magnitude of the planar velocity and change-in-orientation frictions, and are equal to 0.25 and 2 respectively. These formulae have the effect of increasing the planar velocity friction when the ship velocity vector lies in a direction towards the sides of the ship, and decreasing this friction as the velocity vector is more aligned with or directly opposite the forward orientation of the ship.

2.3 Initial signal distribution

At the start of a simulation, a random number of targets is selected from among the possibilities zero, one, two, and three with probabilities 0.1, 0.2, 0.3, and 0.4 respectively. Each target is positioned at a random location in the observation area according to a two-dimensional Gaussian random variable with standard deviation 19.2 (which is the width of the x and y coordinates in the signal domain divided by ten). If two targets are located less than ϵ distance from each other then one is randomly repositioned. Each target is given a uniform random orientation. It has a one third probability to be exhibiting each motion type and the initial velocity is randomly determined based on this motion type. The initial change in orientation is zero for all targets.

3 Observation model

The observations consist of a discrete sequence Y_k of images, each of which is a two-dimensional raster of pixels in a 192 by 192 square. These images are constructed by superimposing figures based on a projection of each target state, $X_{t_k}^i$, onto the raster $R = \{(\ell, m)\}$ and adding noise by the formula

$$Y_k^{(\ell,m)} = \int h^{(\ell,m)}(z)\mathbb{X}_{t_k}(dz) + V_k^{(\ell,m)}, \quad (26)$$

where $V_k^{(\ell,m)}$ is pixel-by-pixel zero-mean independent Gaussian noise with variance $4\cdot(t_k - t_{k-1})$. Here,

$$h^{(\ell,m)}(s) = \begin{cases} 0 & \text{if } (\ell,m) \notin A_s \\ t_k - t_{k-1} & \text{if } (\ell,m) \in A_s \end{cases} \quad (27)$$

for all $s \in S_0$, where A_s is the set of points contained in the filled polygon representation defined by the component projections $\pi_x(s)$, $\pi_y(s)$, and $\pi_\theta(s)$ of s. The shape A_s is described precisely as follows:

- Place a box with sides of length 8 perpendicular to the raster grid and centered at the point $(\pi_x(s), \pi_y(s))$.
- Add a triangle of height 4 to the right side of the box so that the base of the triangle is the side of the box.
- Rotate the resulting polygon by the angle $\pi_\theta(s)$ about $(\pi_x(s), \pi_y(s))$.

The value for ϵ is chosen to ensure that no two such polygons will overlap in the same observation. This procedure creates target sizes that average 80 pixels. The time period for the observations is set to a constant $(t_k - t_{k-1}) = 0.05$ time units, and thus the variance of the Gaussian noise is 0.2. Note that the standard deviation of the noise is approximately 0.447, about 8.944 times the size of the difference in intensity of target versus non-target h values, giving the problem a pixel-by-pixel SNR (signal-to-noise ratio) of $-19.031\,dB$. The observations are not preprocessed; the information from the raster pixels is used directly by the filter algorithm.

4 Filter algorithm

Here we describe the particle-based method by which we solve this nonlinear filtering problem. Our branching particle filter[1, 6] does this, as other particle-based filters[3, 4, 7] do, by approximating the conditional distribution of the signal, given the observations, by a finite sum of measures. In this case, rather than a single Dirac measure being associated with each particle $\mathbb{X}_t^j$, a measure process on (S, d) that, for each time t, is composed of a sum of N_t^j Dirac measures, one for each target $X_t^{i,j}$ within the measure of $\mathbb{X}_t^j$, is associated with each particle. This construction of each particle is identical in form to that of the signal as shown in Equation (6), and at any time t each particle $\mathbb{X}_t^j$ represents a measure in the range of the signal Markov process $\mathbb{X}_t$.

For each new observation, all particles are evolved forward to account for the stochastic dynamics of the signal and then the set of particles is adjusted to account for the information from the observation. In this manner, the particles function as an adaptive Monte-Carlo method for the filtering problem.

The set of particles then approximates the full data of the distribution of the signal conditioned on the set of all back observations. The approximated conditional probability that the signal lies within a given set in the signal domain is computed by dividing the number of particles in that set by the total number of particles.

Particle-based filters require an appropriate algorithm for the adjustment phase such that the filters provably converge to the conditional distribution as the number of particles approaches infinity. In the branching particle-based filter, particles are branched (duplicated or removed) to

form child particles at each observation, with each child particle having the same state in the signal domain as its parent has at the time of the observation. The number of child particles generated (zero, one, or more) is determined by an equation that incorporates the likelihood of the state of each particle given the current observation.

The method is initialized with M particles $\{\mathbb{X}_0^j\}_{j=1}^M$ sampled by the same distribution in the domain of $\mathbb{X}$ as that of the signal, as described in Subsection 2.3. At each observation, the method progresses through the following stages: evolution of the particles, particle branching, and the approximation of the conditional distribution of the signal state. The evolution stage may be amended to incorporate extra particle diffusion, as explained below.

4.1 Evolution

In the evolution stage, each of the particles is evolved independently for the time period between observations $(t_k - t_{k-1})$ according to the Itô equation of the signal, $\mathbb{X}_{t_{k-1}}^j \to \mathbb{X}_{t_k}^j$, as described in Section 2.

4.2 Particle adjustment

After evolving each particle, the particles are then branched to account for the information from the observation. A value labeled $\xi_k^j = \xi(\mathbb{X}_{t_k}^j)$ is calculated for a given particle $\mathbb{X}_{t_k}^j$ in response to the observation at time t_k. The value of ξ is a function that depends on several different parameters, although for a fixed time t_k these parameters are fixed for all particles. The value of ξ depends, for each particle, upon the observation Y_k at time t_k, the distribution of the noise of the observation (V_k as defined in Equation (26)), and the relationship between the the observation and the function h_k from Equation (26). The formula is constructed specifically so that the branching method will provably converge to the optimal filter as the number of particles is increased.

Once ξ is calculated for each particle, each ξ is renormalized to ensure that the expected number of child particles which will be generated, given this particular observation, is equal to the initial number of particles M. Using these renormalized ξ values, each particle is duplicated to form a new particle $\mathbb{X}_{t_k}^* = \mathbb{X}_{t_k}^j$ a number of times equal to $\lfloor(\xi_k^j)^+\rfloor$, and then a uniform-$(0,1)$ random variable U_k^j is generated and

- if $(\xi_k^j - \lfloor(\xi_k^j)^+\rfloor \geq U_k^j)$, an additional particle $\mathbb{X}_{t_k}^*$ with current state value identical to $\mathbb{X}_{t_k}^j$ is added,
- if $(\xi_k^j \leq -U_k^j)$, $\mathbb{X}_{t_k}^j$ is removed, or,
- otherwise, the particle is not branched further.

Intuitively we can interpret ξ_k^j as a measure of the "goodness of fit" of $\mathbb{X}_{t_k}^j$, relative to the other particles, to the hypothesis "$\mathbb{X}_{t_k}^j$ matches the observation Y_k". If this measure is large we duplicate $\mathbb{X}_{t_k}^j$ because it is a "good fit" to Y_k relative to the other particles. If it is near -1 then $\mathbb{X}_{t_k}^j$ is a poor fit relative to the other particles, and we delete the particle. Otherwise, when $\mathbb{X}_{t_k}$ is near 0, the relative "goodness" of the fit is unclear, and we let the particle evolve, hoping for more definitive information in the future.

4.3 Estimation

As discussed in the forthcoming paper by Kouritzin[6],

$$\frac{1}{M}\sum_{j=1}^{M}\mathbb{X}_{t_k}^j(B) \overset{M\to\infty}{\longrightarrow} \int_B p_t^Y(x)dx \tag{28}$$

for Borel subsets B within the signal state space S, where $p_t^Y(x)$ is the conditional distribution of the signal $\mathbb{X}_{t_k}$ given the observations $Y_1, \ldots, Y_k$. Thus, the probability that the signal $\mathbb{X}_{t_k}$ is within the set B at time t_k, conditioned on the observations $Y_1, \ldots, Y_k$, is approximated by the number of particles that are within the set divided by the total number of particles. Such a set B must describe the number of ships (or the set of possible numbers of ships) and the subset of the ship domain that each may occupy.

4.4 Additional particle diffusion

While the branching particle filter approaches the optimal filter as the number of particles increases, for any finite number M of particles the filter may have no particle that matches very well with the signal state. In this case, it is possible that the calculations based on the observations will not cause the filter to generate enough offspring in the correct region of the domain such that one or more child particles diffuse to more closely align with the signal. That is, while the filter is optimal in the limit, the *a priori* distribution of a finite number of particles may be too sparse near the signal state for the diffusion inherent in the evolution stage to draw any particle near to the signal. In this case, the filter does not detect the signal, and will have a poor track which does not properly incorporate all information from the observations.

This problem is particularly acute in multiple target scenarios, in which the signal is composed of multiple objects. Here, the dimensional expansion in the size of the signal domain decreases the likelihood that any one particle will be "close" to the signal in the sense that observation data can usefully adapt particles towards the signal state. If, further, the number of targets is unknown, then a particle can nearly exactly match the signal state for some number of targets but contain too few or too many total targets. In these cases a large number of particles may be required to detect and track the signal, necessitating a commensurate increase in computation.

To somewhat ameliorate this problem it is possible to introduce extra diffusion into the stochastic dynamics that

describe the particle evolution. The idea is described in Ballantyne, Hoffman, and Kouritzin[2] and is similar in approach to simulated annealing. For the ships in the current case, we can perturb each of the x, y, and θ coordinates of each ship by the Gaussian random variable $\mathcal{N}(0, \exp\{-20t_k \cdot (t_k - t_{k-1})\})$ during the evolution associated with an observation at time t_k. Note that the extra diffusion is damped in time so that the filter is still asymptotically optimal.

We simulate the filter both with and without the extra diffusion in order to compare the results obtained.

5 Evaluation

Since no exact optimal filter is constructed, the filter is compared to the simulated signal measure $\mathbb{X}_t$ at each observation time. To calculate a value representing the distance of the filter measure from the actual signal measure at time t_k, we first consider only the set of particles $S = \{\mathbb{X}^j_{t_k} : N^j_{t_k} = N_{t_k}\}$, that is, those which have the same number of targets as the signal. For each of these particles, in the case in which there is a postive number of targets, its distance to the signal measure is computed as follows:

$$||\mathbb{X}_{t_k}, \mathbb{X}^j_{t_k}|| = \min_{\sigma \in perm\{1,..,N_{t_k}\}} \frac{1}{N_{t_k}} \sum_{i=1}^{N_{t_k}} ||X^i_{t_k}, X^{\sigma(i),j}_{t_k}||, \tag{29}$$

where for two ships $s_1, s_2 \in S_0$ we define $||s_1, s_2|| = \Pi(s_1, s_2)$ as in Equation (10), that is, the distance between two ships is taken as the distance in the plane of their (x, y) locations. Here, $X^{\sigma(i),j}_{t_k}$ is the i^{th} target under the permutation σ of the j^{th} particle at time t_k. This formula calculates the average distance between each ship in the signal and its associated ship in the particle under the best possible association.

The value used to represent the distance from the signal of the filter measure is then calculated as

$$\frac{1}{|S|}(1 + \log(\frac{N_{t_k}}{|S|})) \sum_{\mathbb{X}^j_{t_k} \in S} ||\mathbb{X}_{t_k}, \mathbb{X}^j_{t_k}||, \tag{30}$$

where S is the set defined above of particles with the correct number of targets, and the norm $||\mathbb{X}_{t_k}, \mathbb{X}^j_{t_k}||$ above is taken to be 1 for zero-target particles. This introduces a bias to penalize filter estimates that indicate the incorrect number of targets.

The resulting distances are averaged at each time over 400 trials for the filter without extra particle diffusion and 400 trials for the filter with extra diffusion, where the trials complete after 5 time units, which is 100 observations. For each trial, the initial number of particles M_0 is 400000.

6 Results

Figures 2-5 display the penalized average filter positional error for particle evolution simulated with no extra diffusion. The data are broken down to include, for each graph, only the trials in which the signal is initialized with the given number of targets.

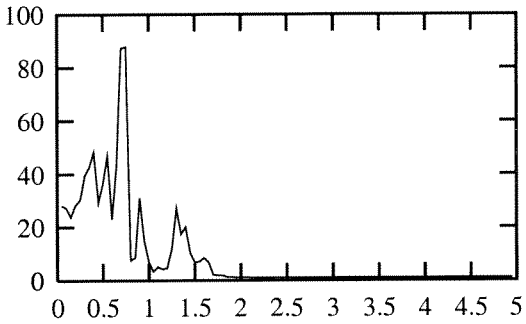

Figure 2: Error in position for zero targets

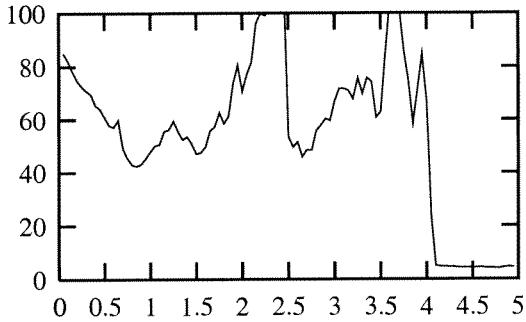

Figure 3: Error in position for one target

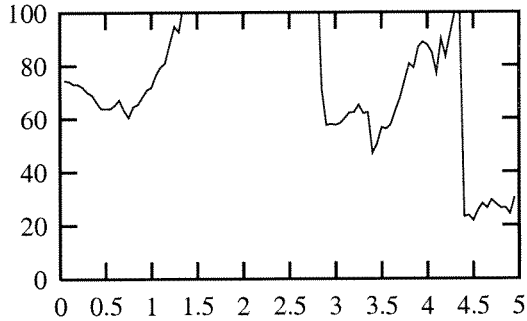

Figure 4: Error in position for two targets

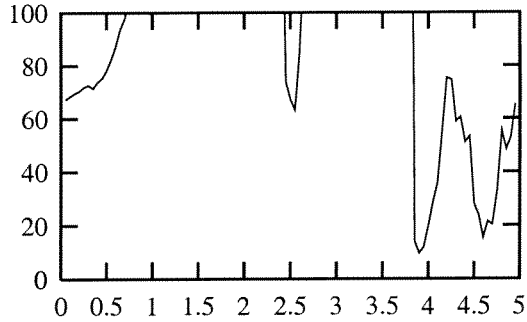

Figure 5: Error in position for three targets

Figures 6-9 display the proportion of particles in the filter that exhibit the correct number of targets, in the case with no extra diffusion, broken down by the initial number of signal targets.

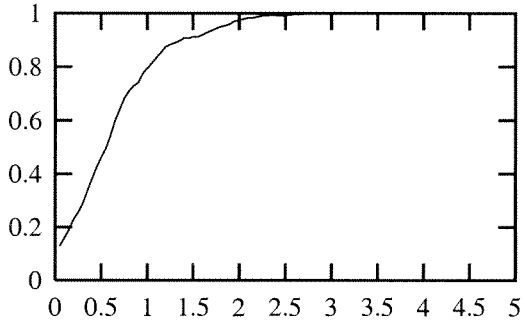

Figure 6: Target number determination for zero targets

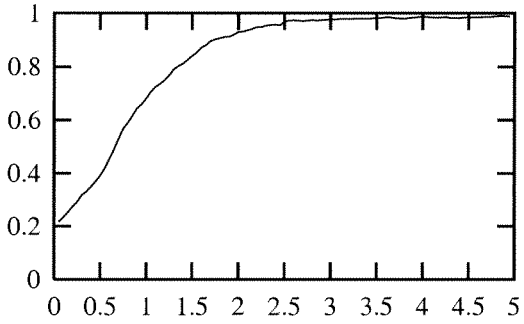

Figure 7: Target number determination for one target

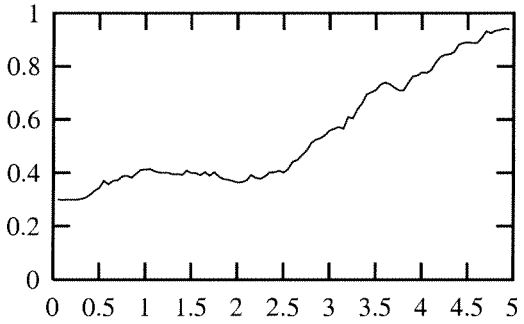

Figure 8: Target number determination for two targets

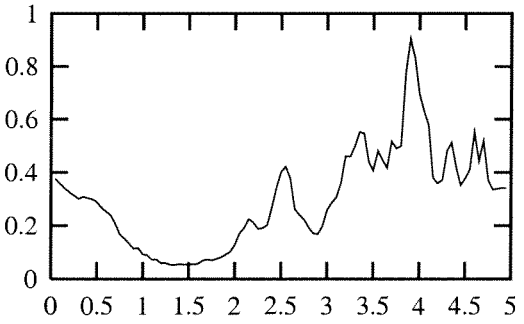

Figure 9: Target number determination for three targets

Figures 10-13 display the penalized average filter positional error for particle evolution simulated with extra diffusion, broken down by the initial number of signal targets.

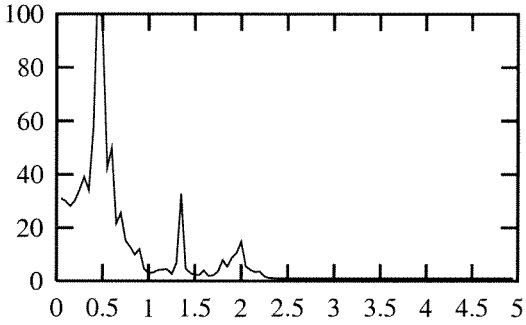

Figure 10: Error in position for zero targets

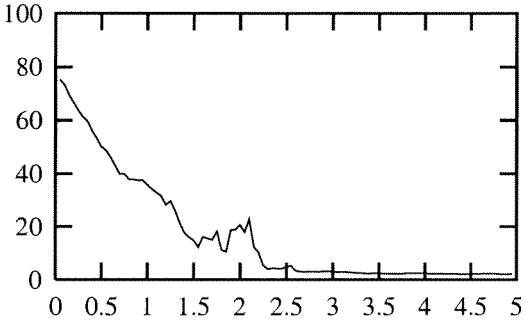

Figure 11: Error in position for one target

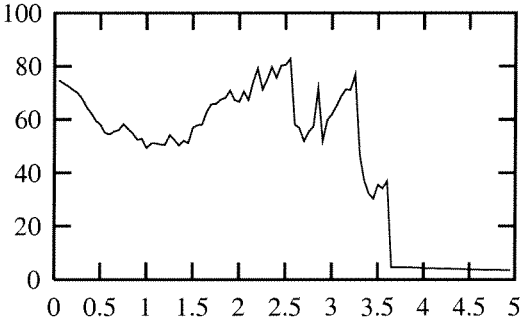

Figure 12: Error in position for two targets

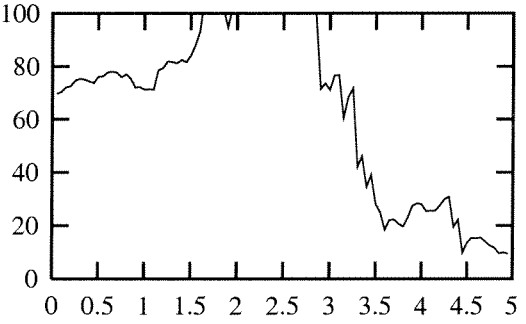

Figure 13: Error in position for three targets

Figures 14-17 display the proportion of particles in the filter that exhibit the correct number of targets, in the case with extra diffusion, broken down by the initial number of signal targets.

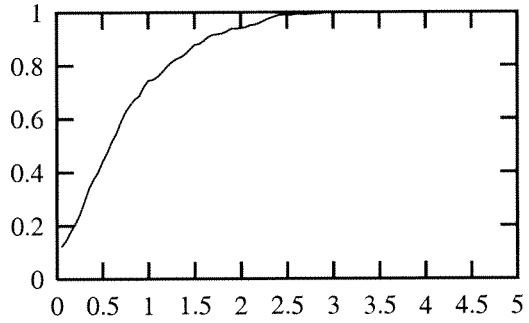

Figure 14: Target number determination for zero targets

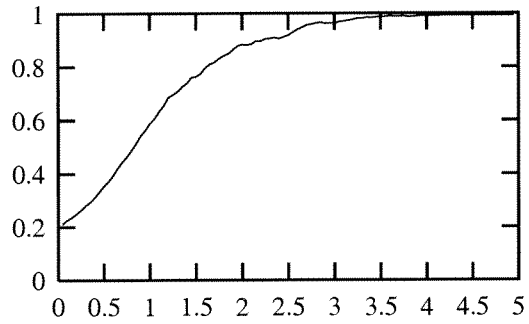

Figure 15: Target number determination for one target

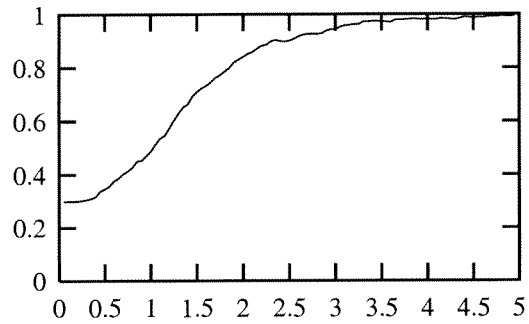

Figure 16: Target number determination for two targets

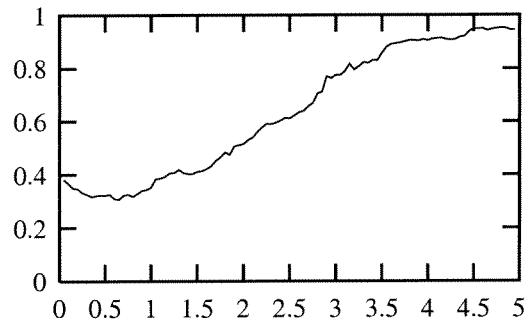

Figure 17: Target number determination for three targets

7 Conclusion

The branching particle-based filter has been found to be effective when extended to estimate the conditional distribution of multi-target signals for unknown, varying, but small numbers of targets. However, the computational resources required to obtain useful results can be large. In the figures above, the standard filter without extra diffusion in the particle evolution exhibited mediocre results in the case of two initial targets and poor results for three initial targets. Simulations with extra particle diffusion indicate a much more successful filter. Therefore, we see that tricks to ameliorate the difficulties inherent in discrete approximations can aid greatly in reducing the computational expense.

8 Acknowledgements

We thank Lockheed Martin, the Pacific Institute for the Mathematical Sciences, and the National Sciences and Engineering Research Council of Canada for their support of this work.

References

[1] D. Ballantyne, H. Chan, and M. Kouritzin, *A novel branching particle method for tracking*, Signal and Data Processing of Small Targets, O. Drummond, SPIE Proc. Vol. 4048, pp. 277-287, 2000.

[2] D. Ballantyne, J. Hoffman, and M. Kouritzin, *Practical application of a branching particle-based nonlinear filter*, Signal Processing, Sensor Fusion, and Target Recognition X, I. Kadar, SPIE Proc. Vol. 4380, 2001.

[3] P. Del Moral and G. Salut, *Non-linear filtering using Monte Carlo particle methods*, C.R. Acad. Sci. Paris, Volume 320, Série I, pp. 1147-1152, 1995.

[4] N. Gordon, *Bayesian methods for tracking*, PhD thesis, Imperial College, University of London, 1994.

[5] C. Hue, J.-P. Le Cadre, P. Pérez, *Tracking multiple objects with particle filtering*, Rapport de Recherche IRISA, No. 1361, October 2000.

[6] M. Kouritzin, *A pathspace branching particle filter*, Preprint.

[7] T. G. Kurtz and J. Xiong, *Particle representations for a class of nonlinear SPDEs*, Stochastic Processes and their Applications, Volume 83, pp. 103-126, 1999.

[8] D. Salmond and N. Gordon, *Group and extended target tracking*, SPIE Proc. Vol. 3809, pp. 284-296, 1999.